energies

Article

Petrophysical and Geochemical Investigation-Based Methodology for Analysis of the Multilithology of the Permian Longtan Formation in Southeastern Sichuan Basin, SW China

Shengqi Zhang [1], Jun Liu [1,*], Li Li [2], Nadhem Kassabi [3] and Essaieb Hamdi [3]

1 Key Laboratory of Deep Underground Science and Engineering (Ministry of Education), Institute of New Energy and Low-Carbon Technology, Sichuan University, Chengdu 610065, China; zsq6149@163.com
2 College of Architecture and Environment, Sichuan University, Chengdu 610065, China; lilill@stu.scu.edu.cn
3 Geotechnical Engineering and Georisks Laboratory (LR14ES03), National Engineering School at Tunis, Université Tunis El Manar, Tunis 1068, Tunisia; kassabi.nadhem.geo@gmail.com (N.K.); essaieb.hamdi@enit.utm.tn (E.H.)
* Correspondence: j.liu@scu.edu.cn

Abstract: Against the backdrop of the national strategic goals of carbon peaking and carbon neutrality, the imperative for China's low-carbon new energy transformation is evident. Emerging as an efficient and clean new energy source, the coal-based "three gases" (coalbed methane, tight sandstone gas, and shale gas) have gained prominence. Nevertheless, the current exploration of the coal-based "three gases" is limited to individual reservoirs, posing challenges to achieving overall extraction efficiency. The primary obstacle lies in the conspicuous disparities in gas content among different reservoirs, with the causes of such disparities remaining elusive. To address this issue, this study focused on the Permian Longtan Formation (coal, shale, and tight sandstone) in the southeastern Sichuan Basin. Through a comparative analysis of the mineral composition, organic geochemical features, and pore structure characteristics, this study aimed to delineate reservoir variations and establish a foundation for the simultaneous exploration and exploitation of the coal-based "three gases". The research findings revealed that the differences in reservoir characteristics account for the variations in gas content among coal, shale, and tight sandstone. The mineral composition of the rock formations in the study area primarily consists of quartz, feldspar, clay minerals, pyrite, calcite, and dolomite. By comparison, the coal samples from the four major coal seams in the study area exhibited relatively large pore sizes, which are favorable for gas accumulation.

Keywords: coal measure gas; shale gas; pore structure; gas content; geochemical properties

check for updates

Citation: Zhang, S.; Liu, J.; Li, L.; Kassabi, N.; Hamdi, E. Petrophysical and Geochemical Investigation-Based Methodology for Analysis of the Multilithology of the Permian Longtan Formation in Southeastern Sichuan Basin, SW China. *Energies* **2024**, *17*, 766. https://doi.org/10.3390/en17040766

Academic Editor: Nikolaos Koukouzas

Received: 29 December 2023
Revised: 2 February 2024
Accepted: 2 February 2024
Published: 6 February 2024

1. Introduction

Coal measures refer to the special rock formations composed of sedimentary rocks that contain coal seams or coal lines [1]. These rock formations are mainly formed in the interplay of land and sea or in a terrestrial environment, often appearing in residual basins with different structural properties [2]. Coal measure gas refers to a diverse range of natural gas resources found within coal measures. It includes coalbed methane, tight sandstone gas, and shale gas (the coal-based "three gases"). These resources are vital components of unconventional gas reserves and exhibit several characteristics that make them significant in the global energy landscape [3]. The global distribution, abundant reserves, homogeneity, and coexistence of coal measure gas resources contribute to their significance in the field of unconventional gas exploration and exploitation. Understanding the characteristics and extraction methods associated with these resources is crucial for maximizing their utilization and contributing to the diversification of the global energy mix [4]. The hydrocarbon source rock matrix contained in the coal measures is the main source for generating these natural gases [5].

Coal measure gas has high scientific and economic value in geological exploration and exploitation. In 2019, China's domestic annual gas production reached 1777×10^8 m^3, while gas imports amounted to 1322×10^8 m^3, resulting in a growing dependence on external gas, which reached 43.1% [6]. Looking ahead to 2030, it is projected that China's domestic annual gas production will increase to 3200×10^8 m^3, with a natural gas consumption of 5500×10^8 m^3 [7]. However, the dependence on external gas is expected to rise to 64% [8]. The increasing dependence on external gas sources reflects the need to secure a stable and diversified supply chain to support the nation's energy requirements. To achieve energy security and sustainability, it becomes imperative for China to enhance domestic gas production capabilities while simultaneously exploring alternative energy sources and implementing strategies to reduce reliance on imports. In 2021, China's coal production reached 4.13 billion tons, accounting for more than 50% of global coal production [9]. China's coal measure gas production is expected to exceed 1000×10^8 m^3 in 2030 [8]. It is an important component of modern energy industries and a crucial part of the natural gas industry. In particular, in China, coal measure gas is considered an important component of future natural gas resources, and its exploration and exploitation have become important tasks in the national energy strategy [10].

The most crucial aspect of studying coal measure gas is to thoroughly investigate the issue of gas content in coalbed gas. In recent years, numerous scholars have been engaged in this research. Sam et al. [11] said key factors affecting gas content variability include gas generation, coal properties, and reservoir conditions. Dai et al. [1] investigated how gas basic parameters and coal quality indexes affect the sorption capacity of coalbed methane. Li et al. [12] analyzed the effects of porosity and permeability on the quality of coalbed methane reservoirs. They found that higher porosity and permeability contribute to higher gas content. Xiao et al. [13] explored the impact of the Protodeacons coefficient of coal samples on the performance of coalbed methane reservoirs. It emphasizes the role of the Protodyakonovs coefficient of coal samples in controlling gas content. Yan et al. [14] analyzed how the pore structure affects coalbed methane production. They found that an increase in temperature enhances gas content. Zhang et al. [15] explored the impact of the TOC, porosity, and thermal maturity on coalbed methane sorption behavior. The results suggest that the TOC, porosity, and thermal maturity are the main factors affecting shale gas accumulation. Zou et al. [16] investigated how coal metamorphism and geological structure influence coalbed methane reservoir performance. They found that stress-induced fractures enhance gas content.

As can be seen from the abovementioned research, after extensive exploration and development practices in oil and gas, it has been realized that the main factors influencing the coalbed gas content include mineral composition, organic geochemical characteristics, and pore structure characteristics [17]. However, there are significant differences in gas content among different formations in the same region [18–20]. For example, the coalbed gas content in the Ordos Basin is 6–10 m^3/t, the shale gas content is 0.2–1.0 m^3/t, and the tight sandstone gas content is 0.1–0.5 m^3/t [8]. The reasons for these differences are still unclear. Therefore, this study focused on the Permian Longtan Formation in the southeastern part of Sichuan Province as the research target to explore the factors causing these differences.

The Permian Longtan Formation, located in the southeastern region of the Sichuan Basin, holds immense importance as a prominent gas-producing basin in China. Within this basin, the southeast depression stands out as a significant area for gas production in the Sichuan Basin. The Permian Longtan Formation exhibits favorable geological characteristics (i.e., high gas content) that contribute to its gas-producing potential, which has attracted substantial attention from the energy industry due to its extensive gas reserves. Accordingly, the main research objectives herein were to investigate the reservoir properties and pore structure, which were characterized using X-ray diffraction (XRD) experiments, high-temperature pump compression tests, rock pyrolysis analysis experiments, vitrinite reflectance, and low-temperature nitrogen adsorption experiments.

Subsequently, based on the comparative evaluation and analysis of different reservoir characteristics, the various reservoir characteristics and gas content were identified in multi-lithology (i.e., coal, shale, and sandstone), providing a theoretical basis for the exploration and development of coal-associated gas in the Permian Longtan Formation in southeastern Sichuan Basin.

2. Geological Background

The Sichuan Basin, situated on the northwestern edge of the Upper Yangtze Craton, is a hydrocarbon-rich basin that extends in a rhombus shape along a northeast direction [21]. The Sichuan Basin boasts abundant high-quality source rocks, characterized by a wide range of strata and extensive mud shale formations that serve as the primary source rock [22]. Additionally, the basin exhibits the presence of developed carbonate source rocks [23].

The Longtan Formation is believed to have been deposited during the Late Cretaceous period, approximately 70 to 85 million years ago, in a marine environment characterized by shallow seas and coastal plains [24]. The sedimentary layers within the Longtan Formation exhibit alternating periods of transgression and regression, reflecting changes in sea level and sedimentation patterns over time [25]. The sandstone beds in the Longtan Formation are well-cemented and often display cross-bedding structures, suggesting deposition by wind or water currents. The shale layers are fine-grained and show laminations, indicating deposition in quiet, low-energy environments. Additionally, the limestone units contain abundant marine fossils, such as mollusks, corals, and foraminifera, which provide valuable insights into the paleoenvironment and paleoclimate of the region.

The research area is located on the western side of the Jiu Dian Ya anticline's western limb, in the middle section of the Sichuan–Hubei–Hunan–Guizhou uplifting fold belt. It is situated on a secondary fold belt developed from the Jian Tou Ya anticline to the Sangmu Chang anticline, forming a radial pattern on a planar distribution, converging towards the northeast and diverging towards the southwest. From east to west, there are four anticlines, namely, the Lianghekou syncline, the Yangchatan anticline, the Mushu syncline, and the Yutiao anticline, which collectively form a westward thrust "dome-shaped structure." This unique structural morphology is the result of the combined and cooperative effects of different directional stresses, causing the uplift of the coal-bearing strata and overlying formations, forming five large-scale fields in the Songzao mining area: Tonghua, Yangtiao, Shihao, Yuyang, and Daluo (Figure 1a).

The coal-bearing strata in the study area belong to the Upper Permian Longtan Formation, which is a transitional zone between marine and terrestrial deposits. The thickness of the coal-bearing strata ranges from 66 to 80 m, with an average thickness of 74 m. The lithology of the strata in the study area consists of gray to dark gray mudstone, sandy mudstone, siltstone, and minor amounts of fine sandstone, mudstone, limestone, and alumina mudstone. There are 10 to 12 coal seams in the strata, with two seams being economically viable and locally viable. The M6-3 and M12 coal seams are locally viable, while the M7 and M8 coal seams are economically viable throughout the entire area (Figure 1b).

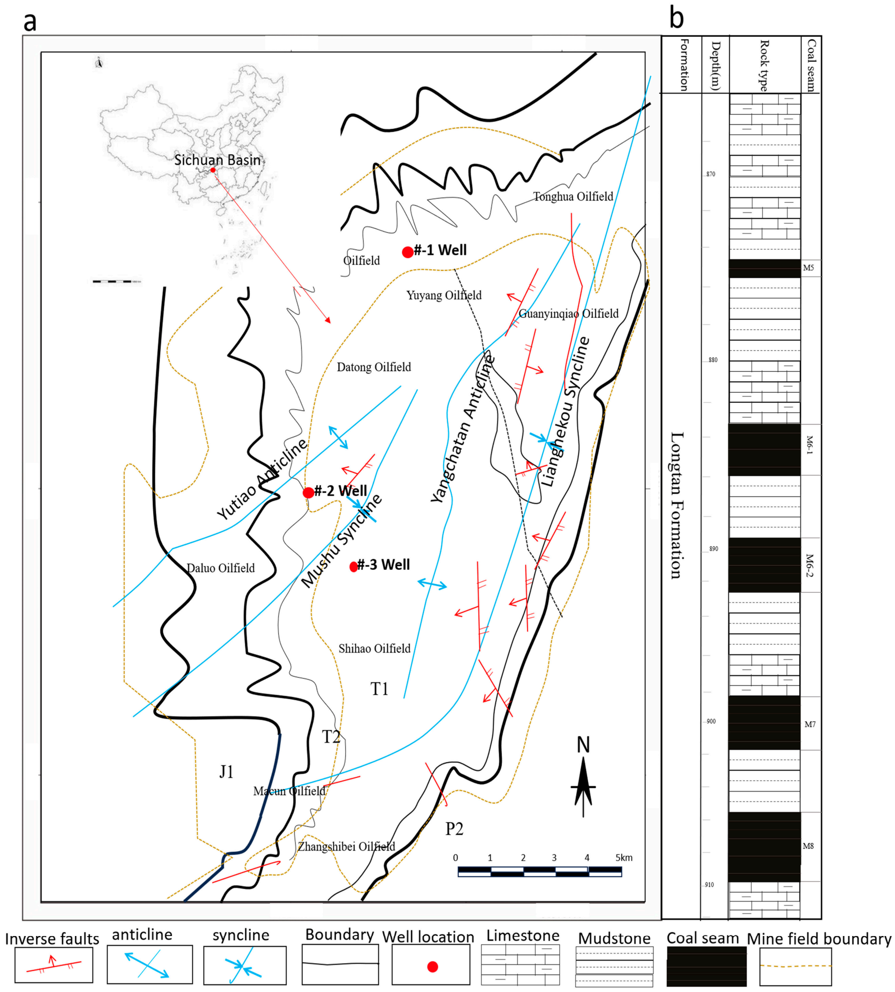

Figure 1. (**a**) Location and geological structure map of the study area. (**b**) Stratigraphic lithology log of the test well.

3. Sampling and Analytical Methods

In the study area, two coalbed methane exploration wells (#-1 and #-2) were implemented, and core samples were obtained using wireline coring. The #-3 well was also implemented, and whole core samples were obtained. The specific locations of the three wells can be seen in Figure 1a. The total thickness of the main coal seams reached 9.35 m in the #-2 well, 6.5 m in the #-1 well, and 5.68 m in the #-3 well. A total of 50 samples were collected from those wells, including arkosic sandstone, coal-bearing rock, mudstone, dolomitic mudstone, marlstone, siltstone, and silty mudstone.

The experimental procedures in this study, as depicted in Figure 2, were conducted to gain insights into the reservoir properties. XRD analysis was employed to determine the mineral composition, focusing on quartz, clay minerals, and carbonate content. These measurements are crucial for understanding the reservoir characteristics. Rock pyrolysis experiments were performed to identify the type and abundance of organic matter using TOC and hydrocarbon generation potential (S_1 + S_2) parameters. This information helps assess the potential for hydrocarbon generation. Vitrinite reflectance experiments provided data on organic maturity, aiding in understanding the thermal history of the reservoir and estimating the timing of hydrocarbon generation. Low-temperature nitrogen adsorption experiments were conducted to characterize the pore structure of the material. Parameters such as pore volume, diameter, and porosity were determined. Pore volume analysis helps understand its storage capacity. Pore size distribution analysis yields information on pore diameter and contributes to assessing permeability and selectivity. Porosity evaluation, indicating the fraction of void space, aids in understanding transport properties. These experiments and subsequent analysis offer a comprehensive understanding of the material's pore structure. Such knowledge is crucial for applications in filtration, catalysis, energy storage, and environmental remediation. These measurements provide insights into the reservoir's storage and flow capacity. Finally, gas content was determined using an on-site analysis method, providing direct quantification of the gas present in the reservoir. Accurate assessment of gas content is vital for estimating reserves and evaluating the economic viability of gas extraction. Overall, these experiments collectively contribute to the understanding of mineral composition, organic matter assessment, maturity evaluation, pore structure characterization, and gas content quantification, facilitating informed decision-making for the extraction of coalbed gas resources. More details regarding these experimental operations are listed in the Supplementary Materials.

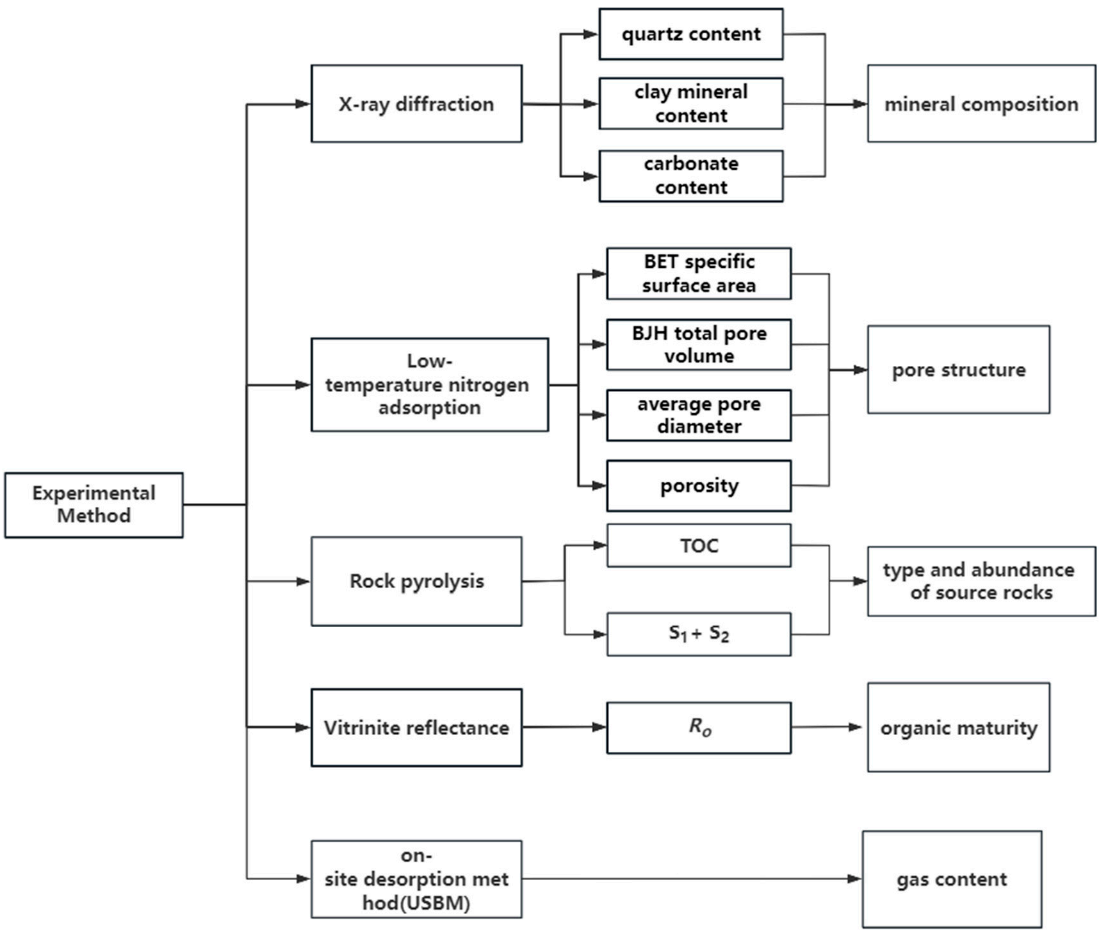

Figure 2. Diagram of parameter and experimental method.

4. Results

4.1. Petrological Characteristics of the Reservoir

The mineral composition results of the study area measured by the XRD experiment are shown in Figure 3. The sandstone in the study area has a quartz content ranging from 11.9% to 31.9%, with an average of 21.1%. The clay mineral content ranges from 14.8% to 57.9%, with an average of 38.0%. The clay minerals herein mainly include kaolinite, illite, montmorillonite, chlorite, and an illite–montmorillonite interlayer. The combined content of feldspar, carbonate, and other minerals ranges from 18.2% to 62.8%, with an average of 40.9%. The other minerals include limited siderite and pyrite. The quartz content in the mudstone ranges from 1.2% to 38.8%, with an average of 15.0%. The clay mineral content ranges from 23.2% to 86.3%, with an average of 56.7%. The combined content of feldspar, carbonate, and other minerals ranges from 10.1% to 66.5%, with an average of 28.2%. The quartz content in the coal seams ranges from 3.9% to 43.1%, with an average of 15.1%. The clay mineral content ranges from 16.1% to 48.6%, with an average of 26.9%. The combined content of feldspar, carbonate, and other minerals ranges from 42.3% to 72.4%, with an average of 58.0%.

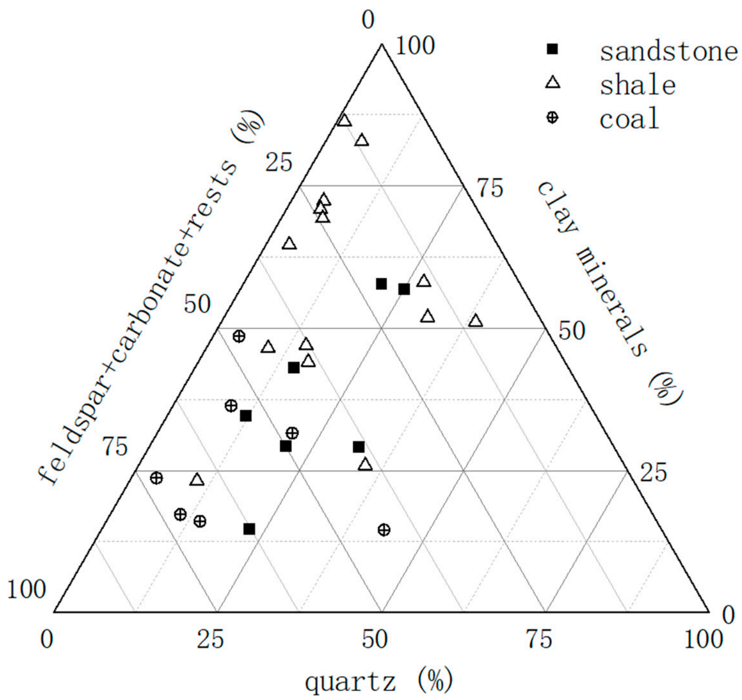

Figure 3. Mineral composition using the XRD method.

Overall, the quartz content is generally less than 50%, and the clay mineral content is relatively high in the shale. Quartz is one of the main minerals in sandstone, mudstone, and coal seams, and its content variation can reflect the physical and genetic characteristics of the rocks. This study found that the quartz content in sandstone, mudstone, and coal seams is generally low, all less than 50%. This characteristic of quartz content is of great significance for the study of coalbed methane geology because it can affect the pore structure, permeability, and gas migration capability of reservoirs. Further research can explore the relationship between quartz content and the storage characteristics of coalbed methane reservoirs through rock physical property tests and gas adsorption experiments [26]. Compared to sandstone and coal seams, shale is relatively rich in clay minerals in its rock composition [27]. The main components of clay minerals include montmorillonite, illite, and kaolinite [28]. This relatively high content of clay minerals may be related to the depositional environment and genesis of shale [29]. Mudstone is often deposited in organic-rich lakes, oceans, or wetland environments, and it is influenced by gravity sedimentation, hydrodynamic action, and chemical precipitation of fine particles [8]. Based on the study of the Longtan Formation shale, we found that the shale of the Longtan Formation exhibits characteristics of high compaction, fine-grained texture, and abundant organic matter. These shales have been deposited in lacustrine, freshwater rivers, or marine environments, influenced by sedimentation from suspended loads, and marine–continental transitional environments [30]. The abundant content of clay minerals can provide excellent storage and adsorption properties for mudstone reservoirs, which have significant influences on the accumulation and release of coalbed gas and shale gas [31].

4.2. Organic Geochemical Characteristics

4.2.1. Organic Matter Abundance

Source rock organic richness is crucial for evaluating its hydrocarbon generation potential. It is commonly assessed by quantifying the abundance of organic matter. This measurement provides insights into the source rock's capacity to produce hydrocarbons. Evaluating organic matter abundance helps determine the overall richness and quality of the source rock as a potential hydrocarbon reservoir. This information is vital for hydrocarbon exploration and production, as it assists in identifying promising areas for further investigation. Thus, characterizing organic matter abundance is essential in source rock evaluation and has significant implications for assessing hydrocarbon resources. Furthermore, organic matter serves as the primary carrier of porosity and plays a significant role in the occurrence of coalbed methane. Typically, parameters such as TOC, chloroform bitumen "A" content, hydrocarbon index (HI), and pyrolysis hydrocarbon potential ($S_1 + S_2$) are employed to assess the organic richness of source rocks. In this study, we utilized two indicators, namely TOC and hydrocarbon potential ($S_1 + S_2$), to evaluate the organic abundance of the coal-bearing reservoir rocks in the research area.

The total organic carbon (TOC) levels of samples collected from the study area exhibited a wide range, spanning from 0.94% to 58.47%, with an average of 22.39%. The TOC levels showed considerable dispersion, as evident from Figure 4. Notably, the coal-bearing rocks displayed higher TOC content, ranging from 31.49% to 58.47%, with an average of 45.91%. In contrast, the shale samples exhibited lower TOC content, varying from 1.2% to 27.92%, with an average of 8.41%. These findings indicate that the coal-bearing rocks in the study area possess a significantly higher TOC content compared to the shale formations. Such variations in TOC content have important implications for hydrocarbon potential and reservoir characterization in the study area. Understanding these differences in organic carbon abundance is crucial for evaluating the source rock's hydrocarbon generation potential and can aid in identifying favorable areas for further exploration and development.

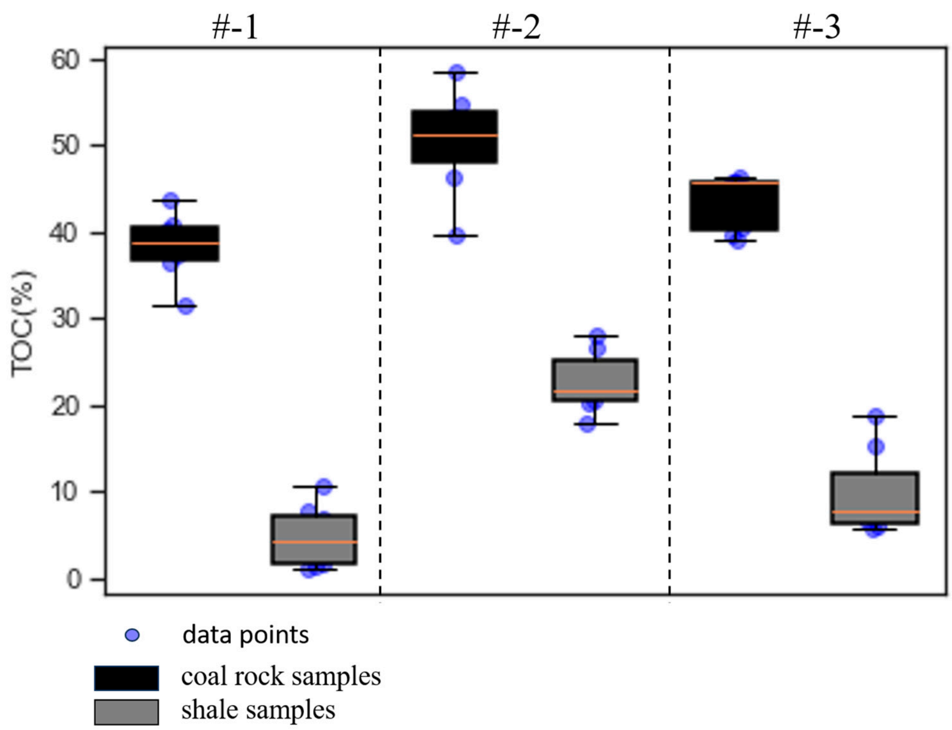

Figure 4. TOC distribution and reservoir comparison chart.

The higher TOC content in coal-bearing rocks compared to shale can be attributed to several factors. Firstly, coal-forming environments are typically characterized by an abundant supply of organic matter, such as plant material, which contributes to the high TOC content in coal. The deposition of organic-rich sediments in swampy environments with stagnant or anoxic conditions promotes the preservation and accumulation of organic material, leading to the formation of coal. In contrast, shale deposition often occurs in marine environments where the organic matter supply may be relatively limited, resulting in lower TOC content.

Secondly, the difference in mineralogy between coal-bearing rocks and shale can also influence TOC content. Coal-forming environments tend to have high proportions of organic matter and lower proportions of mineral matter, allowing for a higher concentration of organic carbon. Shale, on the other hand, contains a higher proportion of mineral matter, such as clay minerals and quartz, which can dilute the organic carbon content and result in lower TOC values.

Finally, variations in the burial history and thermal maturation of the sedimentary rocks can also contribute to the difference in TOC content. Coal-forming processes often involve deeper burial and higher temperatures compared to shale deposition. These higher temperatures during coal formation can cause the release of volatile components from organic matter, resulting in a higher concentration of organic carbon in the remaining coal. Shale, which experiences relatively lower temperatures during burial, may have undergone less thermal maturation, leading to lower TOC content.

The potential hydrocarbon generation amount ($S_1 + S_2$) in the study area exhibited considerable variation. The range spanned from 0.01 to 8.60 mg/g, with an average value of 2.93 mg/g. Notably, a significant majority of the shale samples (approximately 70%) had $S_1 + S_2$ values exceeding 2 mg/g, as observed in Figure 5. In contrast, the coal-bearing rocks displayed a higher range of $S_1 + S_2$ content, ranging from 4.4612 mg/g to 8.5997 mg/g, with an average of 6.1624 mg/g. Conversely, the shale samples exhibited a relatively lower $S_1 + S_2$ content, ranging from 0.1111 mg/g to 0.8474 mg/g, with an average of 0.3229 mg/g. These observations indicate that the coal-bearing rocks in the study area possess a higher potential for hydrocarbon generation compared to the shale formations. This discrepancy can be attributed to the favorable coal formation and preservation environments that facilitate the accumulation of organic matter. The findings contribute to a better understanding of the hydrocarbon potential and resource assessment in the study area, offering valuable insights for future exploration and development strategies.

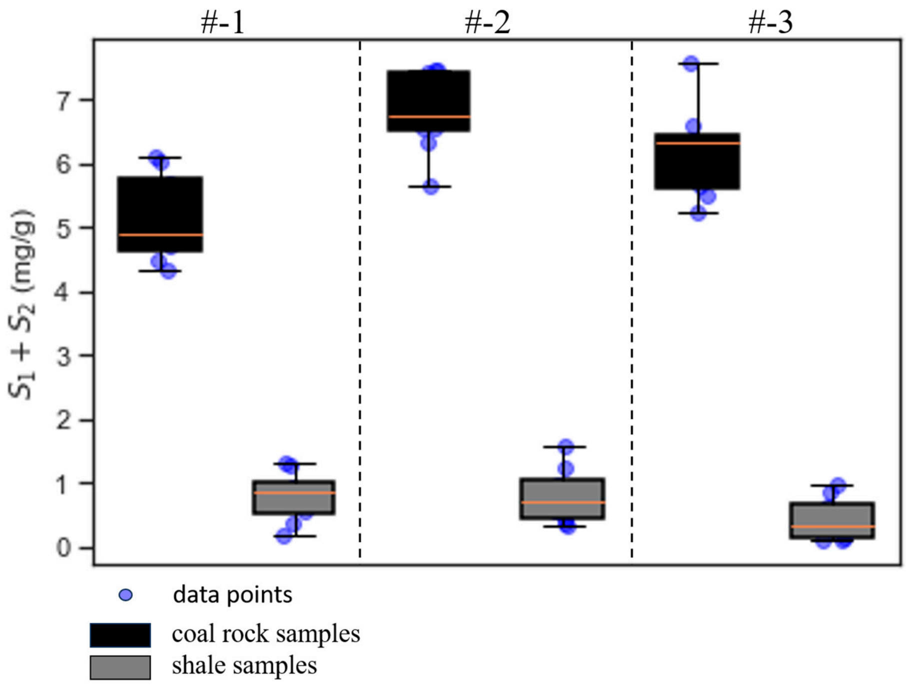

Figure 5. $S_1 + S_2$ distribution and reservoir comparison chart.

4.2.2. Organic Matter Type

The evaluation of organic matter types plays a crucial role in determining the reservoir characteristics and resource potential of coalbed methane. The classification of kerogen is the fundamental method used for assessing organic matter types. Kerogen is classified into three types: Type I, Type II, and Type III [32]. They originate from algal deposits, marine planktonic organisms, and mixed organic matter from microorganisms, as well as higher plants from terrestrial environments. Different types of kerogens exhibit distinct characteristics, with Type I having high oil generation potential, and Type II and Type III having moderate gas generation potential. The hydrogen-to-carbon ratio of Type III kerogen typically ranges from 0.46 to 0.93 [33]. In this study, experimental analyses were conducted using the OG-2000V instrument, and the data were fitted using the Landford et al. model [34], as shown in Figure 6. The results indicated that the coal samples in the study area belong to Type III kerogen.

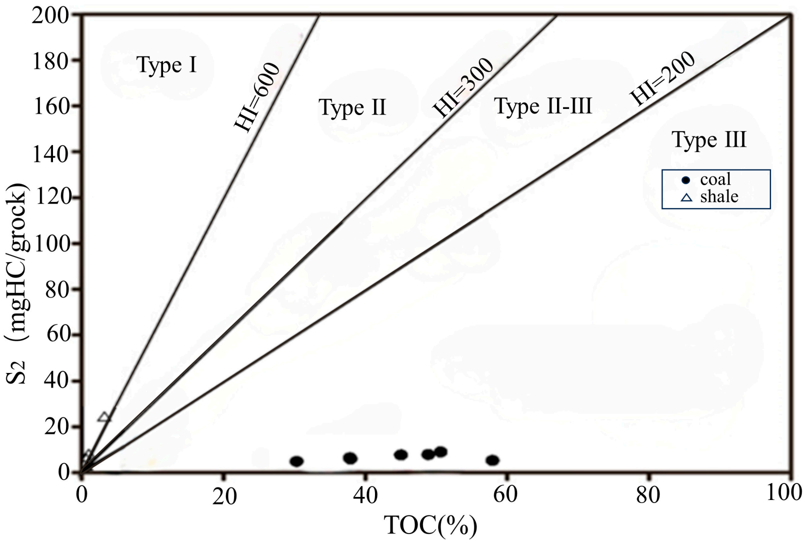

Figure 6. Organic matter type classification chart.

4.2.3. Organic Matter Maturity

Organic matter maturity is a quantitative measure of the thermal evolution of organic matter and serves as an important evaluation indicator of reservoir potential as coalbed gas gradually transitions into gaseous products with increasing thermal evolution. There are several methods available for analyzing organic matter maturity, and this paper utilized techniques such as vitrinite reflectance measurement and rock pyrolysis analysis to investigate organic matter maturity. R_o (vitrinite reflectance) values are widely used as indicators of source rock over-maturity. In this study, the R_o values of 12 samples ranged from 2.28% to 2.57%, with an average value of 2.41%. These R_o measurements provide insights into the level of thermal maturity experienced by the source rocks. The range observed suggests that the samples have undergone moderate thermal alteration. The average $\mathrm{R_o}$ value of 2.25% indicates a consistent level of maturity across the samples. This information is important for understanding the hydrocarbon generation potential and assessing the thermal history of the source rocks. By evaluating R_o values, researchers can make informed decisions regarding the exploration and production of hydrocarbons in the studied area. According to the Terrestrial Source Rocks Hydrocarbon Generation and Evolution Stages Classification and Identification Criteria (SY/T57335-1995) [35], the organic maturity of both the coal and shale in the study area has reached the over-mature stage.

4.3. Pore Structure Characteristics

The low-temperature nitrogen adsorption method involves measuring the adsorption amount at different relative pressures and plotting the adsorption isotherm from the adsorption amount [36]. The nitrogen adsorption value at a relative pressure of 0.98 is converted to the total pore volume, and then the average micropore size and its distribution are calculated using the Horvath–Kawazoe method [37,38].

Based on the low-temperature nitrogen adsorption experiment, the pore volume of the coal seam in the study area ranges from 0.039 cm^3/g to 0.0722 cm^3/g, with an average of 0.0464 cm^3/g, while the pore volume of the shale ranges from 0.0104 cm^3/g to 0.0401 cm^3/g, with an average of 0.0244 cm^3/g, and the pore volume of the sandstone ranges from 0.0171 cm^3/g to 0.0411 cm^3/g, with an average of 0.0251 cm^3/g (Figure 7). It can be seen that the coal seam has a relatively large pore volume. This may be due to the lithological characteristics of the coal seam, which has a higher porosity and a more favorable distribution of pores, resulting in a relatively large pore volume. The composition of coal, primarily consisting of organic matter, undergoes complex processes such as compaction, coalification, and thermal maturation during its formation. These processes result in a denser structure and reduced pore volume within the coal matrix. However, coal-bearing rocks contain larger pores, known as macropores, which are formed during coalification and the release of volatile components. These larger pores contribute to the larger average pore diameter observed in coal-bearing rocks.

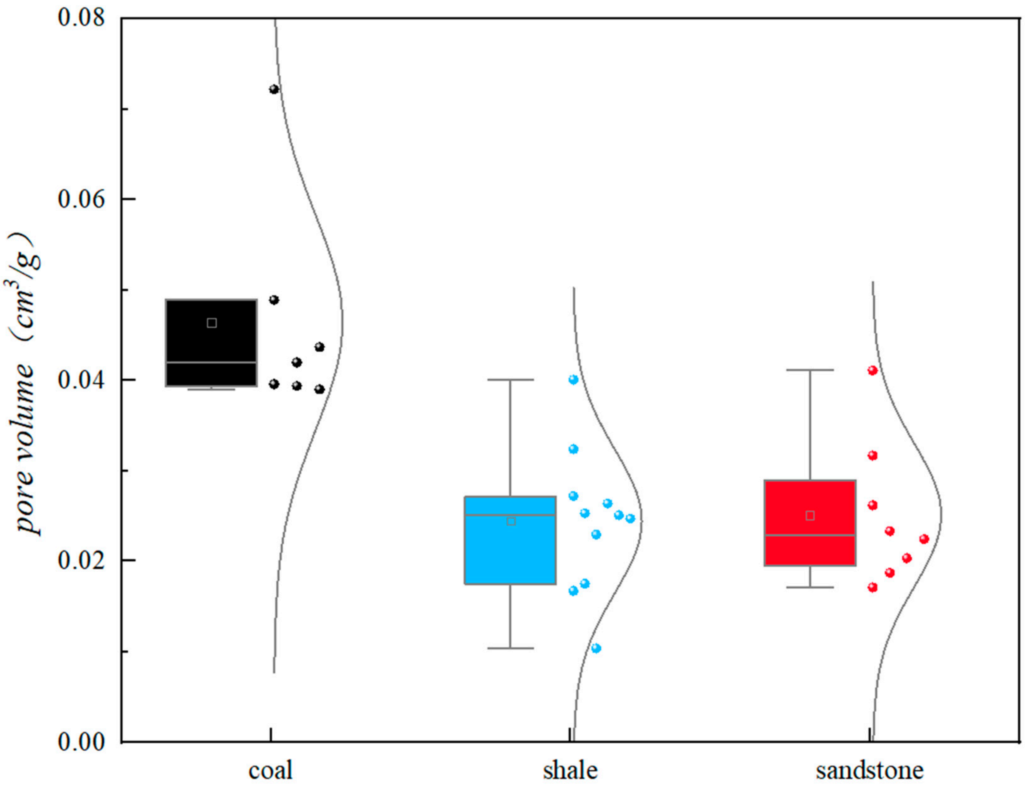

Figure 7. Comparison chart of pore volume distribution.

The average pore size of the coal seam in the study area ranges from 31.4 nm to 54 nm, with an average of 41.7 nm, while the average pore size of the shale ranges from 20.1 nm to 55.6 nm, with an average of 38.0 nm, and the average pore size of the sandstone ranges from 25.9 nm to 74.9 nm, with an average of 39.0 nm (Figure 8). This indicates that the average pore size of shale is relatively small. This may be due to the lithological characteristics of shale, which is subjected to long-term compaction and therefore is limited in the formation and preservation of pores, resulting in a relatively small average pore size. It is worth noting that sandstone has a complex pore structure with a large number of multi-level pores, which may lead to a smaller average pore size. Shale and sandstone are predominantly composed of mineral particles such as clay, quartz, and feldspar. These mineral particles form a framework within the rocks, creating intergranular pores and microfractures that contribute to the overall pore volume. However, it is noteworthy that tight sandstone has larger pore sizes compared to shale. This can be attributed to the differences in the sedimentation and diagenetic processes that shape the pore structure of these rocks. Tight sandstone undergoes more significant compaction and cementation, which can result in pore enlargement and the formation of interconnected pore networks. On the other hand, shale is characterized by finer particles and higher clay content, leading to the formation of smaller-sized pores.

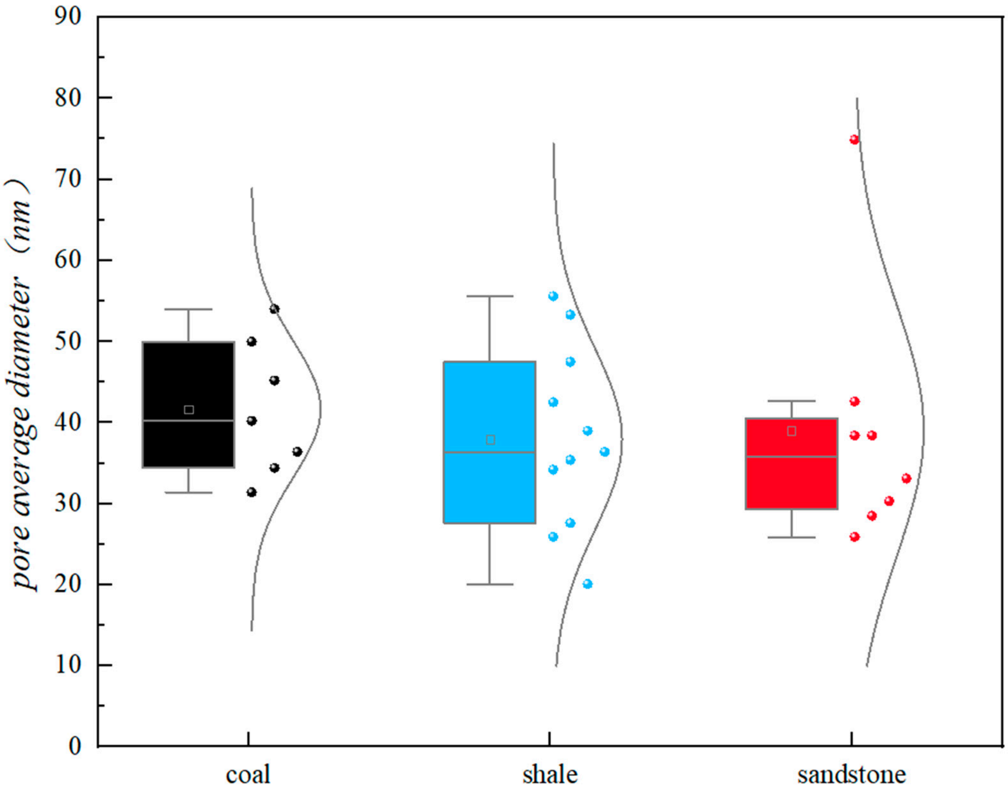

Figure 8. Comparison chart of pore average diameter distribution.

As shown in Figure 9, the porosity of the coal seam in the study area ranges from 6.02% to 8.17%, with an average of 7.13%, while the porosity of the shale ranges from 3.22% to 9.23%, with an average of 5.87%, and the porosity of the sandstone ranges from 4.62% to 9.64%, with an average of 6.66%. It can be seen that the coal seam has a relatively large porosity, while the shale has a relatively small porosity. This may be due to the higher gas content and larger pore structure of the coal seam, resulting in a larger porosity, while the shale is affected by long-term compaction and lithological characteristics, resulting in a smaller porosity.

4.4. Content of Coal Measure Gas

The gas content of the samples was quantified using the methods described in the previous sections. The results, as depicted in Figure 10, revealed a wide range of gas content, ranging from 0.14 cm^3/g to 33.04 cm^3/g, with an average value of 5.25 cm^3/g. Notably, coal-bearing rocks exhibited the highest gas content, followed by shale formations, while tight sandstone samples displayed the lowest gas content. These findings underscore the significant variability in gas content among different lithologies within the study area. The higher gas content observed in coal-bearing rocks indicates their favorable potential as gas reservoirs. Conversely, the lower gas content in tight sandstone suggests limited gas storage capacity. Understanding these variations in gas content is crucial for resource assessment and can guide future exploration and production activities.

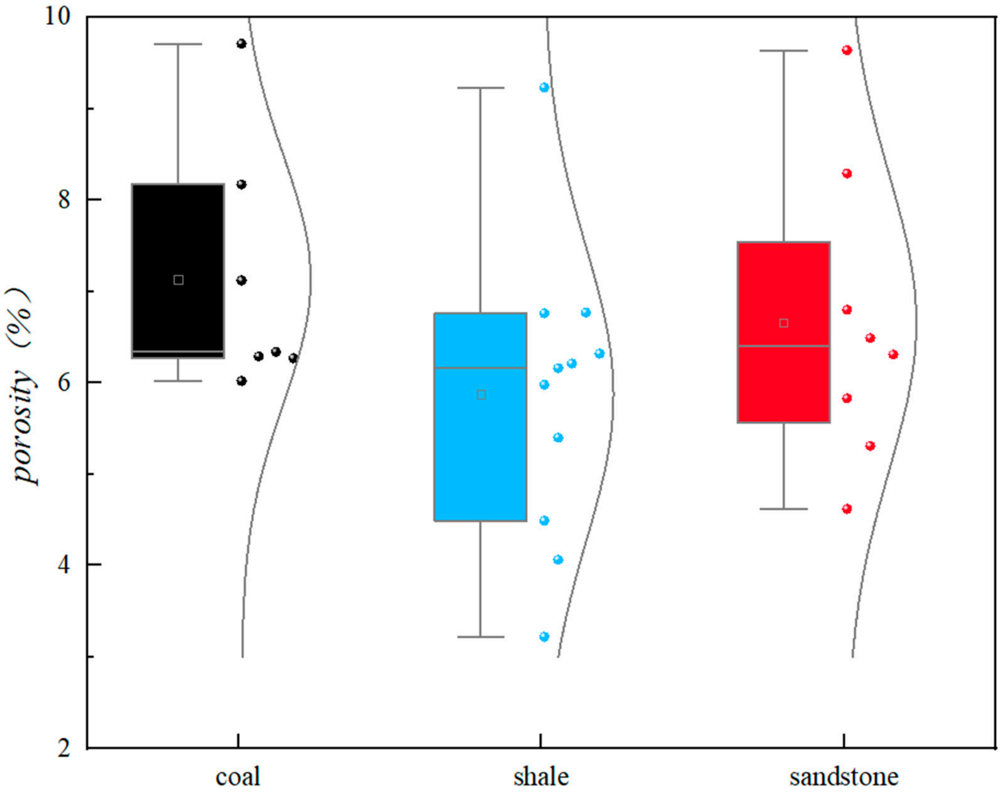

Figure 9. Comparison chart of porosity distribution.

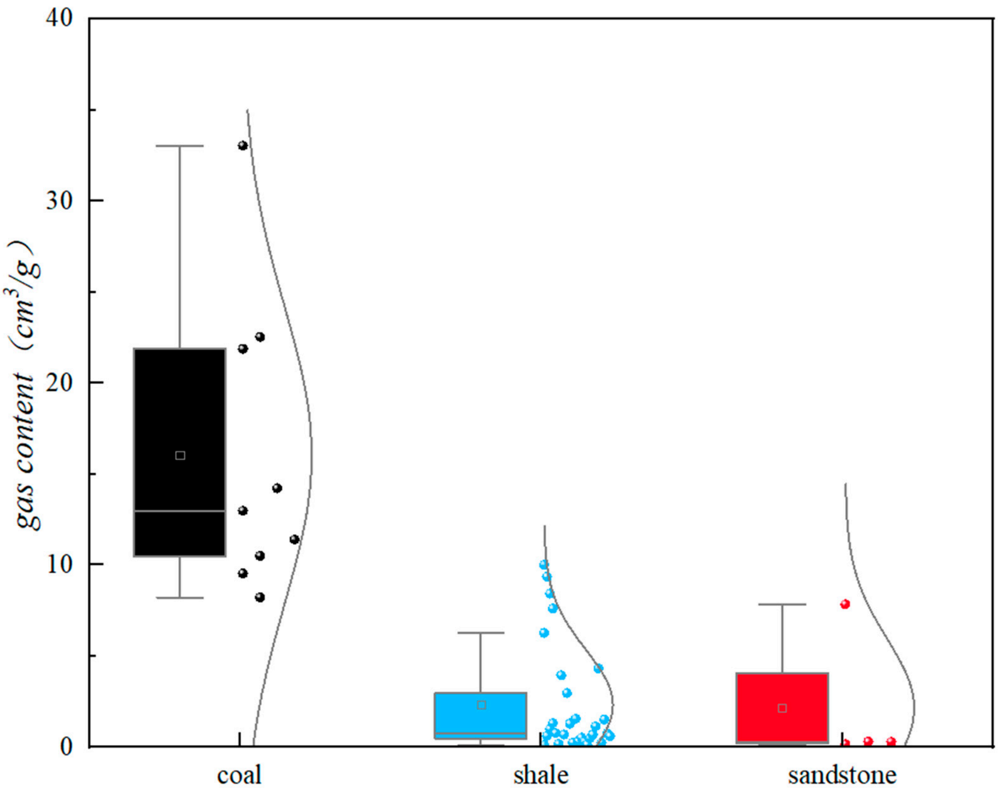

Figure 10. Comparison chart of gas content distribution.

5. Discussion

5.1. Main Controlling Factors of Coalbed Methane

The enrichment and storage of coalbed methane is controlled and influenced by a series of geological factors such as sedimentary conditions, structural conditions, hydrological conditions, stress field conditions, as well as diagenesis and post-coal formation geological processes [39]. At the same time, the occurrence and migration of coalbed methane in coal reservoirs are constrained by various factors such as the coal and rock properties, coal rank, coal pore-fracture system, burial depth, stress state of the strata, and groundwater [40]. Under market economy conditions, the economic feasibility of utilizing coalbed methane as a resource should also be considered. Therefore, the evaluation of coalbed methane resource potential is a comprehensive and systematic assessment involving multiple factors.

(1) Gas content

Gas content is a basic condition that a reservoir must possess and an important indicator for evaluating the quality of coal reservoirs. Generally, the gas content (m^3/t) per unit mass (t) of coal, also known as the in situ gas content, is used to evaluate the gas content of coal reservoirs. Gas content is mainly obtained through on-site drilling and laboratory desorption experiments. The average distribution of coalbed gas content in 105 coal mining areas in China follows a non-normal distribution, with high-gas coal reservoirs dominating: 43 mining areas have a gas content of over 10 m^3/t, accounting for 41%; 29 mining areas have a gas content in the range of 8–10 m^3/t, accounting for 28%; 19 mining areas have a gas content in the range of 6–8 m^3/t, accounting for 18%; and 14 mining areas have a gas content in the range of 4–6 m^3/t, accounting for 13% [41].

Based on the measured gas content in the study area, the lower limit of the gas content that can be extracted is set at 8 m^3/t, which means that areas with a theoretical gas content of less than 8 m^3/t are defined as having no potential for coalbed methane resource development.

(2) Porosity

Compared to conventional oil and gas reservoirs, the contribution of porosity to permeability in coalbed methane reservoirs is relatively small. However, the pore system in coal is still the necessary passage for gas flow, and the degree of pore development still affects the permeability of coalbed methane, especially in the later stages of coal reservoir development. The permeability of coal reservoirs is a function of porosity to the power of three, and the porosity level has a significant impact on the permeability of coal reservoirs. The coal samples from the four main coal seams in the study area have low permeability and belong to low-porosity and low-permeability reservoirs.

5.2. Main Controlling Factors of Shale Gas

The geological work of shale gas in the study area is still in its early stages, and compared to marine shale gas geological features, transitional marine-continental shale has the characteristics of an unstable sedimentary environment, thin single-layer thickness, unstable regional distribution, significant vertical lithological changes, and large variations in organic matter type and content. This study focused on the geological characteristics of transitional marine-continental shale and refer to the evaluation system of marine shale to establish a suitable evaluation system for transitional marine-continental shale gas in the study area.

(1) Total Organic Carbon (TOC)

Organic matter is not only the source of shale gas but also the main adsorbent, directly affecting the accumulation and enrichment of shale gas. The main TOC in the five major shale gas basins in the United States is 0.9% to 3.58%, with an average of 2.87%. The TOC of continental mud shale in China is mainly between 0.58% and 5.16%. Shale gas with industrial value generally has an organic carbon content of no less than 2% [42]. However, considering that the gas-generating capacity of Type III organic matter in transitional marine-continental shale is stronger than Type I and II organic matter, and referring to the standards for TOC in continental and transitional marine-continental shale gas in the "Method for Evaluating Shale Gas Potential and Selecting Favorable Areas for Development" (draft), this study set the lower limit for TOC at 1.0%.

(2) Brittle Mineral Content

Brittle minerals such as quartz, feldspar, and volcanic rock in shale are the main carriers of the shale gas storage space network and play a crucial role in supporting and maintaining the adsorption capacity of shale gas. The higher the content of brittle minerals, the stronger the brittleness of shale, and the better the storage space for shale gas. The content of brittle minerals in shale gas reservoirs is generally above 80% [43]. Based on this, the study set the lower limit of brittle mineral content at 75%.

(3) Thermal Maturity

The thermal maturity of shale is a key factor in the formation and preservation of shale gas. Shale with a higher thermal maturity will have higher gas content and stronger gas-generating capacity. The most widely used index for evaluating thermal maturity is the R_o value, which is a measure of the thermal alteration of organic matter. Shale with a R_o value of 1.6% or above is considered to have good gas-generating potential [44]. In the study area, the average R_o value of the transitional marine-continental shale is 1.7%, indicating a high thermal maturity and good gas-generating potential.

(4) Fracture Density

Fractures are important pathways for gas flow in shale gas reservoirs. The higher the fracture density, the easier it is for gas to flow and the greater the potential for shale gas development. The average fracture density of shale gas reservoirs in the United States is 0.3 fractures/m [45]. Based on this, the study set the lower limit of fracture density at 0.2 fractures/m.

In conclusion, the resource assessment analysis of the study area for coalbed methane and shale gas is a complex and comprehensive task that involves evaluating various geological factors. By considering the gas content, porosity, economic feasibility for coalbed methane, TOC, brittle mineral content, thermal maturity, and fracture density for shale gas, a comprehensive assessment can be made to determine the resource potential for both types of gas in the study area. This information will be valuable for future exploration and development efforts in the region.

5.3. Main Controlling Factors of Gas in Tight Sandstone

Tight sandstone gas, as a significant unconventional natural gas resource, has drawn considerable attention from geologists and engineers. To gain a deeper understanding of the formation and distribution patterns of tight sandstone gas reservoirs, researchers have conducted comprehensive analyses of sedimentary facies, reservoir characteristics, pore structures, diagenetic processes, and diagenetic facies. They have discovered that the formation and distribution of tight sandstone reservoirs are based on the original sedimentary material and controlled macroscopically by different hydrodynamic sedimentary facies. Furthermore, diagenetic processes at the microscopic scale influence the pore structure and permeability of the reservoir, thus impacting its quality.

Reservoir formation is the result of the combined influence of sedimentary facies and diagenetic processes on the original sedimentary material. Although diagenetic processes have a significant impact on the modification of the original porosity of sediments, they occur on the basis of sedimentary processes and are influenced by the sedimentary environment. Consequently, early diagenetic processes are also affected by the sedimentary environment, which further influences the type and intensity of subsequent diagenetic processes and exerts certain control over the pore evolution of sandstones.

Sedimentary facies types directly control the distribution of sand bodies. The thickness of sand bodies generally depends on the stability of the sedimentary environment. When sedimentary conditions, such as hydrodynamic conditions, sediment supply, and sedimentation rate, remain relatively constant, sand bodies tend to be thicker, exhibit better lateral and vertical connectivity, display lower intra-layer heterogeneity, and demonstrate superior grain sorting and well-developed primary porosity. These characteristics contribute to favorable reservoir properties.

In the study area, tests were conducted on lithology, grain size, porosity, permeability, and other relevant properties of tight sandstones within the coal-bearing strata. However, due to the limited number of samples, these test results cannot comprehensively reflect the spatial distribution characteristics of the entire tight sandstone gas reservoir in the study area. Therefore, a comprehensive evaluation of favorable zones for tight sandstone gas was not conducted in this study.

6. Conclusions

Based on the detailed mineral composition analysis of the study area's rock formations, it was found that the main components include quartz, feldspar, clay minerals, pyrite, calcite, and dolomite, among other minerals. Quartz and feldspar are the main brittle minerals, while clay minerals play an important role in rock formations.

In the transitional marine-continental shale of the study area, Type III kerogen predominates. The characteristic of Type III kerogen is its low hydrogen index (HI), indicating a tendency to generate natural gas. This type of kerogen suggests that the shale in the study area may have a high potential for natural gas generation. However, the influence of maturity needs to be considered. Excessive maturity (R_o > 2.5%) would indicate that Type III kerogen has passed its peak period of natural gas generation. Kerogen under high-maturity conditions has already released most of the natural gas, which is unfavorable for the preservation of shale gas. Nevertheless, the shale in the study area still has a high potential for exploitation.

The four main coal seams in the study area exhibited a relatively high porosity, which has a positive impact on gas enrichment. The coal seams in the study area exhibited a high porosity, which is favorable for gas enrichment. These pores provide storage space and pathways for coalbed methane.

Overall, the study area has significant potential for the exploration and development of coal-associated unconventional natural gas, particularly coalbed gas and shale gas. Proper extraction techniques, such as hydraulic fracturing, can help unlock these gas resources and contribute to the energy production in the region.

Supplementary Materials: The following supporting information can be downloaded at: https://www.mdpi.com/article/10.3390/en17040766/s1. About experimental method details. References [46–48] are cited in the supplementary materials.

Author Contributions: Investigation, S.Z.; Data curation, L.L.; Writing—original draft, S.Z.; Writing—review & editing, J.L., N.K. and E.H.; Visualization, L.L.; Supervision, J.L.; Funding acquisition, J.L. All authors have read and agreed to the published version of the manuscript.

Funding: This study was financially supported by the National Key Research and Development Program of China (Grant No. 2022YFE0129800), the National Natural Science Foundation of China (Grant No. 42202204) and the Natural Science Foundation of Chongqing, China (Grant No. CSTB2023NSCQ-LZX0036).

Data Availability Statement: Dataset available on request from the authors.

Conflicts of Interest: The authors declare that the research was conducted in the absence of any commercial or financial relationships that could be construed as a potential conflict of interest.

References

1. Dai, L.; Lei, H.; Cheng, X.; Li, R. Prediction of coal seam gas content based on the correlation between gas basic parameters and coal quality indexes. *Front. Energy Res.* **2023**, *10*, 35–55. [CrossRef]
2. Kang, H.; Gao, F.; Xu, G.; Ren, H. Mechanical behaviors of coal measures and ground control technologies for China's deep coal mines—A review. *J. Rock Mech. Geotech. Eng.* **2023**, *15*, 37–65. [CrossRef]

3. Liu, J.; Bai, X.; Elsworth, D. Evolution of pore systems in low-maturity oil shales during thermal upgrading—Quantified by dynamic SEM and machine learning. *Pet. Sci.* **2024**. [CrossRef]
4. Wang, Y.; Qin, Y.; Yang, L.; Liu, S.; Elsworth, D.; Zhang, R. Organic Geochemical and Petrographic Characteristics of the Coal Measure Source Rocks of Pinghu Formation in the Xihu Sag of the East China Sea Shelf Basin: Implications for Coal Measure Gas Potential. *Acta Geol. Sin.* **2020**, *94*, 364–375. [CrossRef]
5. Wang, X.; Zou, C.; Li, J.; Wei, G.; Chen, J.; Xie, Z.; Li, Z.; Guo, J.; Lin, S.; Pan, S.; et al. Comparison on Rare Gas Geochemical Characteristics and Gas Originations of Kuche and Southwestern Depressions in Tarim Basin, China. *Geofluids* **2019**, *20*, 36–86. [CrossRef]
6. Zhao, Y.; Zhong, H.; Zhang, J.; Nielsen, C.P. Evaluating the effects of China's pollution controls on inter-annual trends and uncertainties of atmospheric mercury emissions. *Atmos. Chem. Phys. Discuss.* **2015**, *15*, 4317–4337. [CrossRef]
7. Hu, Z.; Klitzsch, N.; Jin, Y.; Li, C.; Gong, L.; Li, D.; Wang, S.; Yin, X. Assessment of Shale Gas Potential of Marine-Continental Transitional Longtan Formation from Southwestern Guizhou Province, China. *Energy Fuels* **2023**, *38*, 387–401. [CrossRef]
8. Zhao, W.; Zhang, H.; Shi, Y.; Fu, X.; Hui, J.; Jing, X. Geological characteristics and exploration potential of the coal measure gas from Shan 2 of the Shanxi formation in the eastern Ordos Basin. *Front. Earth Sci.* **2023**, *11*, 35–96. [CrossRef]
9. Tian, W.; Zhao, S.; Tian, F.; Li, X.; Huo, W.; Zhong, G.; Li, S. Symbiotic Combination and Accumulation of Coal Measure Gas in the Daning-Jixian Block, Eastern Margin of Ordos Basin, China. *Energies* **2023**, *16*, 1737. [CrossRef]
10. Fan, C.; Xu, L.; Elsworth, D.; Luo, M.; Liu, T.; Li, S.; Zhou, L.; Su, W. Spatial-Temporal Evolution and Countermeasures for Coal and Gas Outbursts Represented as a Dynamic System. *Rock Mech. Rock Eng.* **2023**, *60*, 37–56. [CrossRef]
11. Boggs, S.J. *Petrology of Sedimentary Rocks*; Cambridge University Press: New York, NY, USA, 2009.
12. Li, P.; Zhang, X.; Li, J.; Zhao, J.; Huang, J.; Zhang, S.; Zhou, S. Analysis of the Key Factors Affecting the Productivity of Coalbed Methane Wells: A Case Study of a High-Rank Coal Reservoir in the Central and Southern Qinshui Basin, China. *ACS Omega* **2020**, *5*, 28012–28026. [CrossRef] [PubMed]
13. Xiao, P.; Liu, X.; Zhao, B. Experimental study on gas adsorption characteristics of coals under different Protodyakonov's coefficient. *Energy Rep.* **2022**, *8*, 10614–10623. [CrossRef]
14. Yan, M.; Bai, Y.; Li, S.; Lin, H.; Yan, D.; Shu, C. Factors influencing the gas adsorption thermodynamic characteristics of low-rank coal. *Fuel* **2019**, *248*, 117–126. [CrossRef]
15. Zhang, Y.; He, Z.; Jiang, S.; Lu, S.; Xiao, D.; Chen, G.; Zhao, J. Factors Affecting Shale Gas Accumulation in Overmature Shales Case Study from Lower Cambrian Shale in Western Sichuan Basin, South China. *Energy Fuels* **2018**, *32*, 3003–3012. [CrossRef]
16. Zou, Z.; Liu, D.; Cai, Y.; Wang, Y.; Li, J. Geological Factors and Reservoir Properties Affecting the Gas Content of Coal Seams in the Gujiao Area, Northwest Qinshui Basin, China. *Energies* **2018**, *11*, 1044. [CrossRef]
17. Fan, C.; Yang, L.; Sun, H.; Luo, M.; Zhou, L.; Yang, Z.; Li, S. Recent Advances and Perspectives of CO_2-Enhanced Coalbed Methane: Experimental, Modeling, and Technological Development. *Energy Fuels* **2023**, *37*, 3371–3412. [CrossRef]
18. Wang, M.; Lun, Z.; Zhao, C.; Wang, H.; Luo, C.; Fu, X.; Li, C.; Zhang, D. Influences of Primary Moisture on Methane Adsorption within Lower Silurian Longmaxi Shales in the Sichuan Basin, China. *Energy Fuels* **2020**, *34*, 10810–10824. [CrossRef]
19. Min, L.; Huaichang, W.; Yan, L.; Weibo, Z.; Huijuan, G.; Hui, Z.; Yunpeng, W. Hydrocarbon generation from confined pyrolysis of Xujiahe Formation coal in the northwest Sichuan Basin, China. *IOP Conf. Ser. Earth Environ. Sci.* **2020**, *600*, 2011–2021.
20. Zhang, H.; Hu, Z.; Xu, Y.; Fu, X.; Li, W.; Zhang, D. Impacts of Long-Term Exposure to Supercritical Carbon Dioxide on Physicochemical Properties and Adsorption and Desorption Capabilities of Moisture-Equilibrated Coals. *Energy Fuels* **2021**, *35*, 12270–12287. [CrossRef]
21. Bian, C.; Zhao, W.; Wang, H.; Chen, Z.; Wang, Z.; Liu, G.; Zhao, C.; Wang, Y.; Xu, Z.; Li, Y.; et al. Contribution of moderate overall coal-bearing basin uplift to tight sand gas accumulation: Case study of the Xujiahe Formation in the Sichuan Basin and the Upper Paleozoic in the Ordos Basin, China. *Pet. Sci.* **2015**, *12*, 218–231. [CrossRef]
22. Dai, J.; Gong, D.; Ni, Y.; Huang, S.; Wu, W. Stable carbon isotopes of coal-derived gases sourced from the Mesozoic coal measures in China. *Org. Geochem.* **2014**, *74*, 123–142. [CrossRef]
23. Yang, Y.; Li, Y.; Zhang, W.; Li, Q.; Long, H. The timing of gas accumulation in the Xujiahe Formation of western Luzhou, Sichuan Basin. *Nat. Gas Ind.* **2010**, *30*, 19–22.
24. Peng, Y.; Guo, S.; Ma, X. Evaluation on the Paralic Shale Gas of Longtan Formation in Guizhou. *Spec. Oil Gas Reserv.* **2018**, *25*, 7–11.
25. Luo, Q.; Xiao, Z.; Dong, C.; Ye, X.; Li, H.; Zhang, Y.; Ma, Y.; Ma, L.; Xu, Y. The geochemical characteristics and gas potential of the Longtan formation in the eastern Sichuan Basin, China. *Pet. Sci. Technol.* **2019**, *179*, 1102–1113. [CrossRef]
26. Fu, H.; Zha, H.; Zeng, L.; Gao, Q. Disintegration behavior and mechanism of carbonaceous mudstone under acidic corrosion and wetting-drying cycles. *Bull. Eng. Geol. Environ.* **2023**, *82*, 35–96. [CrossRef]
27. Narita, A.; Yamada, T.; Matsumoto, M. Platanoid leaves from Cenomanian to Turonian Mikasa Formation, northern Japan and their mode of occurrence. *Paleontol. Res.* **2008**, *12*, 81–88. [CrossRef]
28. Kheir, S.A.; Bamford, B.; Brogiato, A.; Carli, G.D.; Lambrughi, A. Assessment of the creep behavior of siltstone for the Snowy 2.0 hydropower station using multistage uniaxial creep tests. *IOP Conf. Ser. Earth Environ. Sci.* **2023**, *1124*, 012003. [CrossRef]
29. Yang, P.; Miao, S.; Wang, H.; Li, C.; Shang, X.; Xia, D. Comparison of deformation behavior between creep and fatigue on siltstone and its modified damage model. *Int. J. Fatigue* **2023**, *46*, 3815–3828. [CrossRef]

30. Wang, E.; Guo, T.; Li, M.; Xiong, L.; Dong, X.; Zhang, N.; Wang, T. Depositional Environment Variation and Organic Matter Accumulation Mechanism of Marine-Continental Transitional Shale in the Upper Permian Longtan Formation, Sichuan Basin, SW China. *ACS Earth Space Chem.* **2022**, *6*, 2199–2214. [CrossRef]
31. Yu, T.; Huang, Q.; Kang, X.; Liu, X.; Xie, Q. On seismic response of loess-mudstone slope with underlying anti-dip fault zone: Laboratory investigation using shaking table test. *Bull. Eng. Geol. Environ.* **2023**, *82*, 38–43. [CrossRef]
32. Chen, L.; Wang, Z.; Xie, Y.; Huang, W. Organic matter types of the Early Paleogene from the Sanshui Basin and its response to paleoclimate. In Proceedings of the 1st International Conference on Energy and Environmental Protection (ICEEP 2012), Hohhot, China, 23–24 June 2012; pp. 5809–5812.
33. Jia, Y.; Han, D.; Wang, C.; Zhang, J.; Su, M. *Organic Matter Type Judging Method, Involves Obtaining Content Percentage of Organic Micro-Component, and Judging Organic Matter Type of Sample According to Content Percentage of Organic Micro-Component*; University Yangtze: Jingzhou City, China, 2013; pp. 35–75.
34. Kang, S.; Shao, L.; Qin, L.; Li, S.; Liu, J.; Shen, W.; Chen, X.; Eriksson, K.A.; Zhou, Q. Hydrocarbon Generation Potential and Depositional Setting of Eocene Oil-Prone Coaly Source Rocks in the Xihu Sag, East China Sea Shelf Basin. *Acs Omega* **2020**, *5*, 32267–32285. [CrossRef]
35. Huang, F.; Xin, M.A. *Geochemical Evaluation Method of Nonmarine Source Rocks*; China National Petroleum Corporation: Beijing, China, 1995; pp. 1–10.
36. Qi, L.; Tang, X.; Wang, Z.; Peng, X. Pore characterization of different types of coal from coal and gas outburst disaster sites using low temperature nitrogen adsorption approach. *Int. J. Min. Sci. Technol.* **2017**, *27*, 371–377. [CrossRef]
37. Ni, G.; Li, S.; Rahman, S.; Xun, M.; Wang, H.; Xu, Y.; Xie, H. Effect of nitric acid on the pore structure and fractal characteristics of coal based on the low-temperature nitrogen adsorption method. *Powder Technol.* **2020**, *367*, 506–516. [CrossRef]
38. Ren, Z.; Jia, B.; Zhang, G.; Fu, X.; Wang, Z.; Wang, P.; Lv, L. Study on adsorption of ammonia nitrogen by iron-loaded activated carbon from low temperature wastewater. *Chemosphere* **2021**, *262*, 12–95. [CrossRef] [PubMed]
39. Tao, S.; Pan, Z.J.; Tang, S.L.; Chen, S.D. Current status and geological conditions for the applicability of CBM drilling technologies in China: A review. *Int. J. Coal Geol.* **2019**, *202*, 95–108. [CrossRef]
40. Pan, J.N.; Ge, T.Y.; Liu, W.Q.; Wang, K.; Wang, X.L.; Mou, P.W.; Wu, W.; Niu, Y.B. Organic matter provenance and accumulation of transitional facies coal and mudstone in Yangquan, China: Insights from petrology and geochemistry. *J. Nat. Gas Sci. Eng.* **2021**, *94*, 24–36. [CrossRef]
41. Ye, J.C.; Tao, S.; Zhao, S.P.; Li, S.; Chen, S.D.; Cui, Y. Characteristics of methane adsorption/desorption heat and energy with respect to coal rank. *J. Nat. Gas Sci. Eng.* **2022**, *99*, 23–41. [CrossRef]
42. Ge, T.Y.; Pan, J.N.; Wang, K.; Liu, W.Q.; Mou, P.W.; Wang, X.L. Heterogeneity of pore structure of late Paleozoic transitional facies coal-bearing shale in the Southern North China and its main controlling factors. *Mar. Pet. Geol.* **2020**, *122*, 66–85. [CrossRef]
43. Li, M.; Li, M.J.; Pan, J.N.; Gao, D.; Cao, Y.X. Coalbed methane accumulation, in-situ stress, and permeability of coal reservoirs in a complex structural region (Fukang area) of the southern Junggar Basin, China. *Front. Earth Sci.* **2023**, *10*, 45–96. [CrossRef]
44. Men, X.Y.; Tao, S.; Liu, Z.X.; Tian, W.G.; Chen, S.D. Experimental study on gas mass transfer process in a heterogeneous coal reservoir. *Front. Earth Sci.* **2021**, *216*, 75–96. [CrossRef]
45. Tao, S.; Chen, S.D.; Pan, Z.J. Current status, challenges, and policy suggestions for coalbed methane industry development in China: A review. *Energy Sci. Eng.* **2019**, *7*, 1059–1074. [CrossRef]
46. Fu, X.; Qin, Y.; Wang, G.G.X.; Rudolph, V. Evaluation of gas content of coalbed methane reservoirs with the aid of geophysical logging technology. *Fuel* **2009**, *88*, 2269–2277. [CrossRef]
47. Cook, H.E. Method of sample prepare and X-ray diffraction data analysis. *Natl. Conf.* **1984**, *28*, 41–411.
48. Otia, C. Vitrinite reflectance as maturity parameter. *ACS Sym.* **1996**, *62*, 63–85.